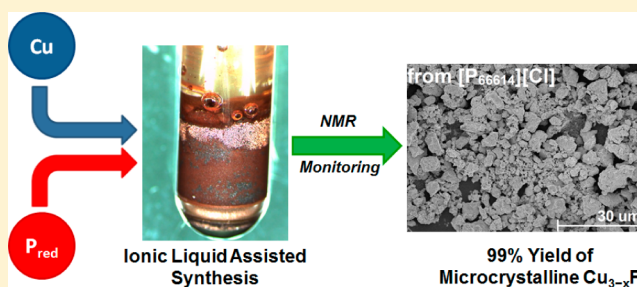


Resource-Efficient High-Yield Ionothermal Synthesis of Microcrystalline  $\text{Cu}_{3-x}\text{P}$ Alexander Wolff,<sup>†</sup> Julia Pallmann,<sup>†</sup> Richard Boucher,<sup>‡</sup> Alexander Weiz,<sup>†</sup> Eike Brunner,<sup>†</sup> Thomas Doert,<sup>\*,†</sup> and Michael Ruck<sup>†,‡</sup><sup>†</sup>Department of Chemistry and Food Chemistry and <sup>‡</sup>Department of Material Science, Technische Universität Dresden, 01062 Dresden, Germany<sup>#</sup>Max Planck Institute for Chemical Physics of Solids, 01187 Dresden, Germany

## S Supporting Information

**ABSTRACT:** Polycrystalline  $\text{Cu}_{3-x}\text{P}$  was successfully synthesized in different ionic liquids comprising imidazolium and phosphonium cations. The reaction of elemental copper and red phosphorus in trihexyltetradecylphosphonium chloride at 200 °C led to single-phase  $\text{Cu}_{3-x}\text{P}$  ( $x = 0.05$ ) within 24 h with a quantitative yield (99%). Liquid-state nuclear magnetic resonance spectroscopy of the ionic liquids revealed degeneration of the imidazolium cations under the synthesis conditions, while phosphonium cations remain stable. The solid products were characterized with X-ray powder diffraction, scanning electron microscopy, energy-dispersive X-ray spectroscopy, solid-state nuclear magnetic resonance spectroscopy, and elemental analysis. A reinvestigation of the electronic transport properties of  $\text{Cu}_{2.95(4)}\text{P}$  showed metallic behavior for the bulk material. The formation of  $\text{CuP}_2$  during the synthesis of phosphorus-rich  $\text{Cu}_{3-x}\text{P}$  ( $x \geq 0.1$ ) was observed.



## INTRODUCTION

In the past decade the scientific community has begun to consider phosphorus to be a limited resource.<sup>1–3</sup> Phosphorus, as a key element for living cells, plays a major role in food production. Approximately 80% of the globally mined phosphate rock is used for the production of fertilizers.<sup>4</sup> While other critical resources, such as natural oil or gas, may become replaceable, this is not the case for phosphorus.<sup>5,6</sup> Thus, the waste of phosphorus should rigorously be reduced, even in the production of inorganic phosphorus-containing materials.

One class of phosphorus-containing compounds is the binary metal phosphides, which have a wide variety of structures, interesting properties, and technical uses.<sup>7–9</sup> They have been studied intensively, for instance, as catalytic materials.<sup>10–13</sup> The optical properties of  $\text{Zn}_3\text{P}_2$  can be used in photovoltaic applications.<sup>14–16</sup> Even superconductivity has been discovered in the metal-rich molybdenum phosphides  $\text{Mo}_3\text{P}$ ,  $\text{Mo}_8\text{P}_5$ , and  $\text{Mo}_4\text{P}_3$ .<sup>17</sup> The main-group compounds  $\text{InP}$  and  $\text{GaP}$  are well-known semiconductors used in several applications, for example, as light-emitting diodes.<sup>18,19</sup>

The compound commonly referred to as  $\text{Cu}_3\text{P}$  is a deoxidizer for copper alloys and a sintering additive in metallurgy.<sup>20–23</sup> It also has, along with other metal or semimetal phosphides, attracted attention as a potential candidate for anodes in lithium ion batteries.<sup>24–26</sup> The crystal structure of  $\text{Cu}_3\text{P}$  was described in 1972 by Olofsson.<sup>27</sup> His investigations as well as later work by Schlenger et al. revealed a homogeneity range

between approximately  $\text{Cu}_{2.90}\text{P}$  and  $\text{Cu}_{2.75}\text{P}$ .<sup>27,28</sup> The copper deficit is accompanied by vacancies at two of the four crystallographic copper positions in the structure.<sup>27</sup> Recently, de Trizio et al. identified the 6c Wyckoff positions as being most favorable for vacancies based on density functional theory (DFT) calculations.<sup>29</sup> They concluded that vacancies should form even in  $\text{Cu}_3\text{P}$ , which agrees with the intrinsic sub-stoichiometric nature of this compound as proposed by Schlenger et al. and Olofsson.<sup>27,28</sup> On this basis it seems appropriate to generally refer to this compound as  $\text{Cu}_{3-x}\text{P}$ . It has been suggested that these vacancies are the origin of the specific plasmon dynamics of  $\text{Cu}_{3-x}\text{P}$ .<sup>29,30</sup>

There are different reports about the band gap of  $\text{Cu}_{3-x}\text{P}$  in literature. According to optical<sup>31</sup> and scanning tunneling spectroscopy,<sup>30</sup> the gap is found between 0.8 and 1.3 eV. Recently, *p*-type semiconducting behavior was claimed for  $\text{Cu}_{3-x}\text{P}$  nanoparticles.<sup>32</sup> However, observations of comparatively low electrical resistance<sup>33</sup> and a Knight shift as well as Korringa-type behavior of the spin–lattice relaxation rate in solid-state nuclear magnetic resonance (NMR) spectroscopy<sup>34</sup> indicate that the bulk material is metallic in nature.

In previous works, crystalline  $\text{Cu}_{3-x}\text{P}$  was synthesized by the direct reaction of the elements copper and red phosphorus in sealed silica tubes at 560 °C for at least 5 d.<sup>28</sup> Typically byproducts, such as  $\text{Cu}$  or  $\text{CuP}_2$ , depending on the ratio of the

Received: June 9, 2016

Published: August 25, 2016

starting materials, were also obtained. To overcome this problem, surface solid-state reactions were developed. In this type of reaction, red phosphorus is suspended, e.g. in ethanol, and then sprayed on a copper foil.<sup>24,35</sup> The foil is fired at temperatures of  $T \geq 250$  °C, leading to the formation of  $\text{Cu}_{3-x}\text{P}$  on the surface.<sup>25</sup> The powder can then be scratched off in order to obtain the product, however, the yield is limited by the surface area of the copper foil. Another production route involves a mechanochemical approach based on ball milling. However, in addition to the presence of impurities, e.g. WC, from the milling balls,<sup>26</sup> the crystallinity of the product is rather poor and an additional heat treatment may be necessary.<sup>35</sup> Subsequently, solvothermal syntheses were developed as a more convenient route for obtaining high quality  $\text{Cu}_{3-x}\text{P}$  material. The respective starting materials and reaction conditions are listed in Table 1. In this kind of synthesis, the

**Table 1. Selected Solvothermal Syntheses of Crystalline  $\text{Cu}_{3-x}\text{P}$**

starting materials	conditions	solvent	ref
CuCl, TOP <sup>a</sup>	350 °C, 0.8 h	OLA <sup>b</sup> , ocytlamine	29,32
CuCl, PH <sub>3</sub>	230 °C, 0.25 h	OLA, TOPO <sup>c</sup>	30
Cu, P <sub>white</sub>	220 °C, 2 h	octadecene/toluene	36
CuCl <sub>2</sub> ·2H <sub>2</sub> O, P <sub>white</sub>	140 °C, 10 h	aqueous NH <sub>3</sub>	37
CuSO <sub>4</sub> ·5H <sub>2</sub> O, P <sub>white</sub>	180 °C, 12 h	glycol/ethanol/water	39
CuCl <sub>2</sub> ·2H <sub>2</sub> O, P <sub>white</sub>	140 °C, 12 h	ethylenediamin	38
Cu, P <sub>red</sub>	190 °C, 10 h	ethylenediamin	35
Cu, P <sub>red</sub>	200 °C, 24 h	H <sub>2</sub> O	31
CuCl, P <sub>red</sub>	200 °C, 24 h	H <sub>2</sub> O	31
CuCl <sub>2</sub> , P <sub>red</sub>	200 °C, 24 h	H <sub>2</sub> O	31
CuI, P <sub>red</sub>	200 °C, 24 h	H <sub>2</sub> O	31

<sup>a</sup>Trioctylphosphine. <sup>b</sup>Oleylamine. <sup>c</sup>Trioctylphosphine oxide.

choice of the starting material is essential. For example, nucleation has to be controlled during the synthesis of nanoparticles. Therefore, at least one precursor must be sufficiently soluble in order to achieve this control. This was accomplished by using toxic phosphorus reagents like phosphane<sup>30</sup> or white phosphorus<sup>36</sup> as well as with different copper precursors.<sup>29,30,32,36</sup> During the synthesis of nanoparticles, a substitution of this toxic reagent with trioctylphosphine<sup>29,32</sup> was feasible, but the temperature had to be increased to achieve decomposition of the phosphorus precursor. Especially during the synthesis of bulk material with white phosphorus, a considerable excess had to be used to obtain single-phase products.<sup>37–39</sup>

$\text{Cu}_{3-x}\text{P}$  powders were also successfully synthesized using nontoxic red phosphorus.<sup>31,35</sup> Aitken et al. showed that replacement of ethylenediamine by pure H<sub>2</sub>O as the solvent had beneficial effects on the synthesis. In their approach various copper precursors were employed; however, a sizable excess of red phosphorus was necessary in all cases. The smallest excess (2 equivalents) was needed for the reaction with CuCl, and the largest excess had to be used for the reaction with copper metal (30 equiv.).

Here we report a convenient and resource-efficient route to synthesize microcrystalline  $\text{Cu}_{3-x}\text{P}$  from nontoxic red phosphorus at low temperatures with a very high yield, which should also be up-scalable for industrial processes. This method combines a relatively short reaction time and the pressureless setup of ionothermal<sup>40–44</sup> syntheses with the high atomic efficiency of solid-state reactions.

## EXPERIMENTAL SECTION

**Starting Materials.** The ionic liquids (ILs) 1-butyl-3-methylimidazolium chloride ([BMIm][Cl], IoLiTec, 99%) and trihexyltetradecylphosphonium chloride ([P<sub>66614</sub>][Cl], CYPHOS, 95%) were dried at 110 °C for 12 h under vacuum. Copper (ABCR, 99.9%, spherical, 100 mesh) was treated with H<sub>2</sub> at 400 °C before use. Following a procedure described by Brauer et al., red phosphorus (ABCR, 99.999%) was washed with sodium hydroxide, rinsed with refluxing water, and finally dried in vacuum.<sup>45</sup>

**Synthesis.** All compounds were handled in an argon-filled glovebox (M. Braun;  $p(\text{O}_2)/p^0 < 1$  ppm,  $p(\text{H}_2\text{O})/p^0 < 1$  ppm). In a typical synthesis, 381 mg (6.00 mmol) of copper and 63 mg (2.03 mmol) of red phosphorus were carefully weighed directly into a glass flask with a magnetic stirring bar (final ratio Cu/P = 2.95:1). Note that any loss of phosphorus, which is a sticky powder, causes impurities of unreacted copper in the product, whereas an excess of it leads to impurities of CuP<sub>2</sub>. The starting materials were covered with either 1310 mg (7.5 mmol) of [BMIm][Cl] or 1298 mg (2.5 mmol) of [P<sub>66614</sub>][Cl]. The flask was closed with a glass stopper and subsequently placed in an oil bath. The flask was quickly heated to 200 °C and then stirred vigorously. After the mixture was stirred for 24 h, the flask was removed from the bath and allowed to cool to room temperature. To isolate the product the mixture was dispersed in ethanol (96%), centrifuged (4400 rpm), and then redispersed in fresh ethanol with the help of ultrasound. This procedure was repeated three times. Afterward the obtained powder was dried in air at 60 °C for 12 h. According to powder X-ray analysis and energy-dispersive X-ray (EDX) spectroscopy, single-phase samples of Cu<sub>2.95(4)P</sub> are obtained with yields of 372 mg (84%) for [BMIm][Cl] and 438 mg (99%) for [P<sub>66614</sub>][Cl].

**Elemental Analysis.** For the elemental analysis of Cu, P, Cl, C, O, and Na, combinations of different methods were used. The analysis of Cu, P, and Na was made with inductively coupled plasma atomic emission spectroscopy using a 5100 SVDV (Agilent). A C200 CHLH (LECO) was used for the detection of organic carbon (combustion method). The oxygen content was probed with the carrier gas hot extraction method using a TCH 600 (LECO). The chloride analysis was made using the combustion ion chromatography method (AQF-2100, Mitsubishi).

**Powder X-ray Diffraction.** Powder X-ray diffraction (PXRD) was performed at 296(1) K on an X'Pert Pro MPD diffractometer (PANalytical) equipped with a curved Ge(111) monochromator by using Cu K $\alpha_1$  radiation ( $\lambda = 154.056$  pm). Le Bail analysis was done within the software package Jana2006<sup>46</sup> using an internal LaB<sub>6</sub> standard (660b, National Institute of Standards and Technology, USA).

**Scanning Electron Microscopy.** The dried as-prepared samples were dispersed in ethanol, and a few drops were placed on polished silicon wafers. After evaporation of the ethanol, the wafers were fixed on a sample holder with a graphite pad. Scanning electron microscopy (SEM) was performed by using an SU8020 instrument (Hitachi) with a triple detector system for secondary and low-energy backscattered electrons ( $U_e = 3$  kV).

**Energy-Dispersive X-ray Analysis.** The samples were pressed into pellets with a diameter of 6 mm under vacuum with a load of 2 tons. The pellets were then embedded under vacuum into an epoxy polymer in which graphite was dispersed. Afterward, the pellets were wet-ground with a MetaServ 250 (Buehler, silicon carbide grinding paper) and subsequently polished with a VibroMet 2 (Buehler, MasterPrep alumina suspension 0.05  $\mu\text{m}$ ). The polished pellets were finally fixed on the sample holders with a graphite pad. The compositions of the samples were determined by quantitative EDX ( $U_e = 20$  kV) analysis using an SU8020 instrument (Hitachi) equipped with a Silicon Drift Detector X-Max<sup>N</sup> (Oxford). In light of the preparation method, the elements C and O (both part of the polymer) and Al (from polishing suspension) were omitted in EDX quantifications.

**Nuclear Magnetic Resonance Spectroscopy.** All liquid-state NMR experiments were performed using an Avance 400 (Bruker)

spectrometer at 348(2) K. The samples were transferred into tubes with polytetrafluoroethylene valves (Deutero) in an argon-filled glovebox. The pure ILs were dried before use as described above; the reacted ILs were transferred into the glovebox without exposure to air. The  $^{31}\text{P}$  NMR spectra were recorded at a resonance frequency of 161.98 MHz, and the  $^1\text{H}$  NMR spectra were recorded at a resonance frequency of 400.13 MHz by using a 5 mm high-resolution probe. A pulse length of 16  $\mu\text{s}$  at 14 W ( $^{31}\text{P}$ ) and 10.15  $\mu\text{s}$  at 20 W ( $^1\text{H}$ ) and relaxation delays of 2 s ( $^{31}\text{P}$ ) and 1 s ( $^1\text{H}$ ) were used. The chemical shifts were referenced relative to  $\text{H}_3\text{PO}_4$  for  $^{31}\text{P}$  NMR measurements and relative to tetramethylsilane for  $^1\text{H}$  NMR measurements. Magic angle spinning (MAS) NMR experiments were performed on a Bruker Avance 300 spectrometer using a commercial double-resonance 2.5 mm MAS NMR probe operating at a resonance frequency of 121.5 MHz and a MAS frequency of 16 kHz. For these measurements the phosphorus chemical shifts were referenced relative to  $\text{H}_3\text{PO}_4$ . For the determination of the chemical shift of signals in the  $^{31}\text{P}$  MAS NMR spectra, the center of gravity of the signals was used.

**Quantum Chemical Calculations.** Scalar-relativistic DFT calculations were performed in the Elk code,<sup>47</sup> which is based on the full-potential linearized augmented plane-wave method within the local-density approximation. A number of full-potential linearized augmented-plane wave basis functions up to  $R_{\text{MT}}K_{\text{max}} = 8$  (where  $R_{\text{MT}}$  is the average radius of the muffin-tin spheres, and  $K_{\text{max}}$  is the maximum value of the wave vector  $K = k + G$ ) were considered and the maximum length of  $G$  for expanding the interstitial density and potential was set to 12. A total number of 16  $k$ -points was obtained in the irreducible part of the Brillouin zone.

**Electrical Resistivity Measurements.** A sample with the composition of  $\text{Cu}_{2.95(4)}\text{P}$  was selected for electrical resistivity measurements. The powder was checked for purity with PXRD and SEM, and the composition was determined by EDX. The fine ground powder was subsequently compacted with spark plasma sintering (SPS) using an SPS-515 ET setup (Fuji Electronic Industrial) under a pressure of 100 MPa with a heating rate of 50 K/min at a temperature of 350  $^\circ\text{C}$  for 10 min. Afterward the pellet was manually broken into pieces and checked for purity by PXRD, SEM, and EDX again. One piece of the pellet was selected for the resistivity measurements. This piece was contacted on a holder using Au wires in a four-point measurement configuration and in a configuration with two pairs of opposing contacts for Hall measurements. Finally, the dependence of the resistance was measured with the sample in He exchange gas between 4 and 300 K.

## RESULTS AND DISCUSSION

**Synthesis.** In a previous work, we observed an unexpected reactivity of red phosphorus with iodine in the IL  $[\text{BMIm}][\text{Cl}]\cdot 2\text{AlCl}_3$ .<sup>48</sup> Subsequent experiments aiming at a targeted synthesis of phosphides showed that a mixture of copper metal and red phosphorus (element ratio 2.95:1) in ILs led to a dark solid product. After the IL was removed with ethanol and the product was dried, a fine greyish powder was obtained. The powder is single-phase  $\text{Cu}_{3-x}\text{P}$  according to PXRD (Figure 1). EDX mapping showed a homogeneous distribution of Cu and P inside the sample (Figure S1, Supporting Information) making the presence of X-ray amorphous red phosphorus improbable. The results of the elemental analysis (Table S1, Supporting Information) exclude residuals of the ILs on the particle surface. Only low amounts of oxygen and chloride contaminations as well as sodium impurities, most probably caused by the used glassware, were found. Closer investigations of the powder with SEM revealed particles, which are inhomogeneous in size and have irregular shapes (Figure 2). The particle sizes range from  $\sim 1\ \mu\text{m}$  to  $15\ \mu\text{m}$ . Interestingly, the cations of the ILs appear not to substantially affect the particle morphology.

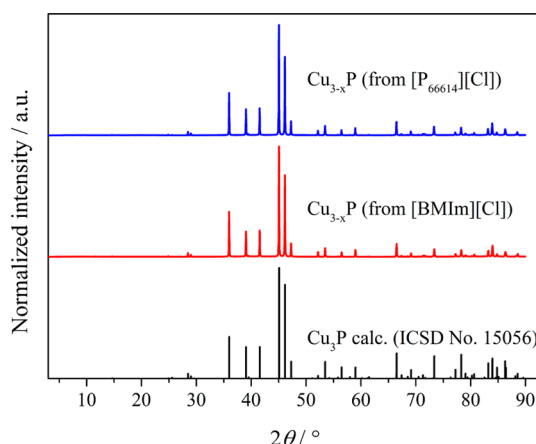


**Figure 1.** PXRD patterns of  $\text{Cu}_{3-x}\text{P}$  from reaction of Cu and  $\text{P}_{\text{red}}$  (2.95:1 molar ratio) in  $[\text{P}_{66614}][\text{Cl}]$  and  $[\text{BMIm}][\text{Cl}]$  vs that calculated on the basis of the Inorganic Crystal Structure Database No. 15056.

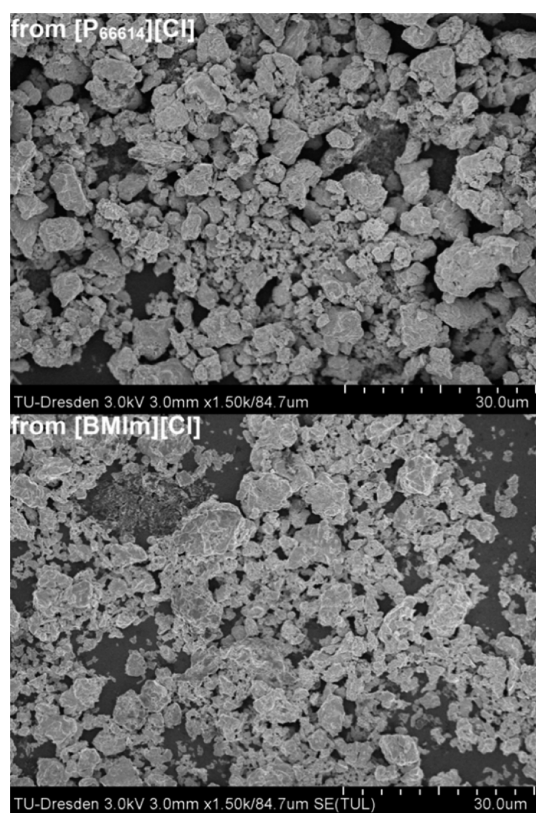


**Figure 2.** SEM images of the as-prepared  $\text{Cu}_{3-x}\text{P}$  (after washing and drying).

In the course of this work, a few conditions that yield an incomplete reaction of the starting materials could be identified. The substitution of the chloride anion of  $[\text{BMIm}][\text{Cl}]$  by bromide or iodide led to a noticeable decrease of the reaction rate, while  $[\text{P}_{66614}][\text{decanoate}]$  or  $[\text{P}_{66614}][\text{bis}(\text{tri-}u\text{oromethyl-sulfonyl})\text{imide}]$  were found to lead to a significant amount of impurities of copper when applying the same reaction conditions. Therefore, it should be considered that chloride anions might play a role during the activation of the starting materials. There are already many examples for the activation of  $\text{P}_{\text{white}}$  by nucleophilic reagents.<sup>49</sup> Recently, nucleophilic loosening of P–P bonds has also been observed with  $\text{P}_{\text{red}}$  in different

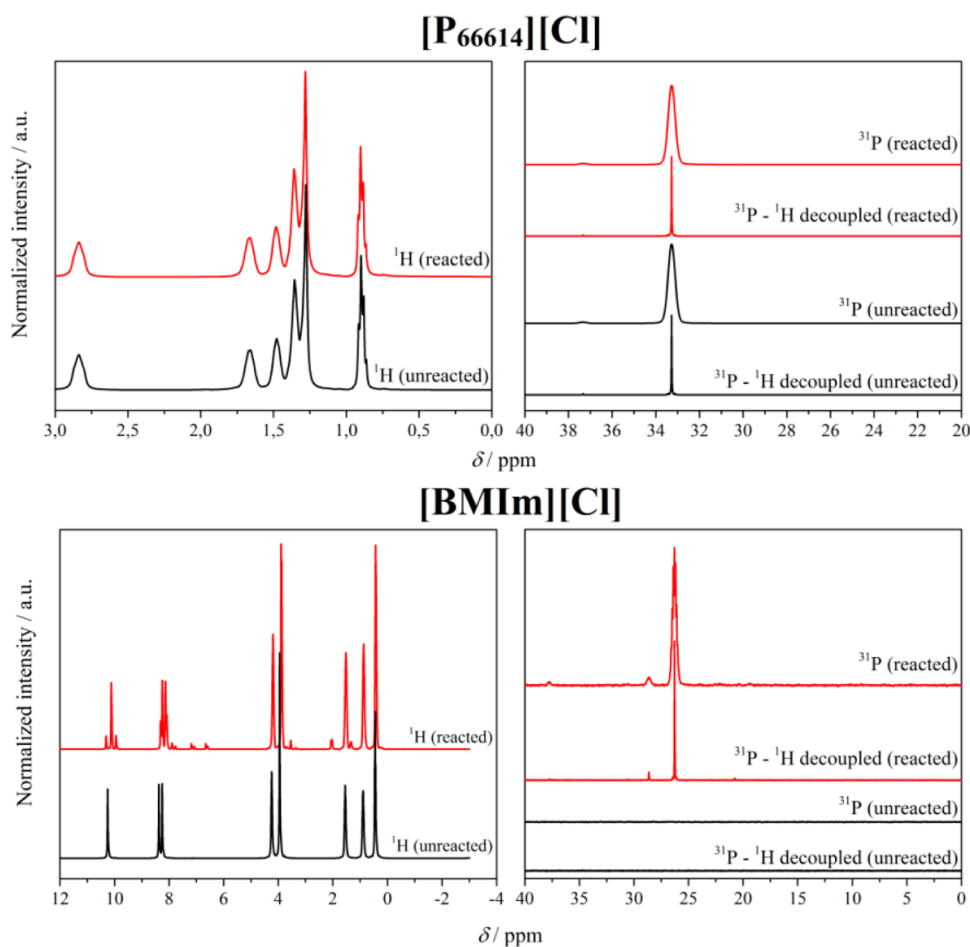


**Figure 3.** Liquid-state  $^1\text{H}$  NMR and  $^{31}\text{P}$  NMR spectra of the ILs before (black lines) and after (red lines) reaction of copper and red phosphorus inside the liquids. For reasons of clarity, only the ranges of the spectra with signals are shown.

organic solvents.<sup>50</sup> Because a decreased reaction rate was observed while lowering the nucleophilicity of the anion, it was assumed that a comparable mechanism might play a role during this synthesis. However, this must be verified in future experiments. Remarkably, replacing metallic copper as the starting material by  $\text{CuCl}$ ,  $\text{CuI}$ , or  $\text{CuCl}_2$  failed and yielded only unidentifiable products with poor crystallinity. Obviously, the copper halides are not appropriate as redox partners for the reduction of the red phosphorus in ILs.

The new synthesis route presented here, although related to the one described by Aitken et al.,<sup>31</sup> shows some major improvements compared to the approaches presented previously. First, the reaction is highly efficient. No excess of phosphorus is needed, and the product yield is high. While the reaction in  $[\text{P}_{66614}][\text{Cl}]$  runs almost quantitatively (yield 99%), side reactions of the phosphorus with the imidazolium cation reduce the yield to 84% in  $[\text{BMIm}][\text{Cl}]$  (see next section). The ILs could be removed easily from the product with a common organic solvent in both cases. This is a great improvement compared to the classic preparation of binary and ternary metal phosphides in metal fluxes, for example, Sn, because a treatment with hydrochloric acid is no longer needed.<sup>51</sup> The second advantage of this synthesis route arises from the fact that ILs are generally not volatile.<sup>52</sup> The experimental procedure can be heavily simplified; no pressure control or autoclave are needed. Instead, the reaction can be conducted in a common glass flask, as neither solvent nor starting materials

generate autogenous pressure. This illustrates another advantage of red phosphorus. In addition to its nontoxicity, it does not develop a significant vapor pressure below 400 °C (in contrast to, for example, white phosphorus or  $\text{PH}_3$ ).<sup>53</sup> Moreover, the flask allows for vigorous stirring, which easily leads to comparatively short reaction times. As shown in this work, inert conditions are needed to suppress side reactions with oxygen or moisture, which can be achieved by sealing the flask with a simple glass stopper. An upscaling of the reactions seems only limited by the size of the reaction flask and the strength of the stirring mechanism.

**Reaction Studies with Liquid-State Nuclear Magnetic Resonance Spectroscopy.** To obtain more detailed insights into the reaction pathway, liquid-state NMR experiments with  $^1\text{H}$  and  $^{31}\text{P}$  nuclei were performed, Figure 3. In practice, two different reaction paths should be considered. First, phosphorus may react with copper to form a soluble complex that decomposes at elevated temperatures to form the final product  $\text{Cu}_{3-x}\text{P}$ . In this case, additional signals of the dissolved species should appear in the  $^{31}\text{P}$  NMR spectrum. Second, phosphorus could simply diffuse into copper in a similar way as observed for common solid-state reactions. The second scenario has already been observed for solvothermal synthesis of nanocrystalline  $\text{Cu}_{3-x}\text{P}$ <sup>29,32</sup> and other metal-rich phosphide nanoparticles.<sup>54</sup>

In our experiments, the ILs were measured before use as well as after the reaction. No changes in the NMR spectra of  $[\text{P}_{66614}][\text{Cl}]$  (Figure 3, top) were detected, which supports the

latter pathway in accordance with literature results.<sup>29,32,36,54</sup> However, the exact mechanism and the question of whether the IL contributes to the activation of the reactive species must be investigated in more detail in the future. The fact that no degeneration of the  $[P_{66614}]$  cation occurred is probably one reason for the almost quantitative yield of  $Cu_{3-x}P$  from this reaction. In contrast, numerous additional signals are detected in the  $^1H$  and  $^{31}P$  NMR spectra when conducting the same reaction in  $[BMIm][Cl]$  (Figure 3, bottom). Differences in the spectra highlight a degeneration of the imidazolium cation through the reaction with phosphorus. Interestingly, the PXRD analysis (Figure 1) does not show any copper impurities in the  $Cu_{3-x}P$  product. Most likely, the phosphorus species detected in the  $^{31}P$  NMR are coordinated by copper ions, an assumption that is also supported by the considerably lower product yield as compared to the reaction in  $[P_{66614}][Cl]$ . As the type of organic cation does not seem to have any influence on the particle morphology (Figure 2), degeneration of the cation is not expected to affect the reaction path itself but lead to a loss of starting materials instead. This is probably the reason for the reduced product yield that we observed for reactions in  $[BMIm][Cl]$ . Consequently, a precise control of the stoichiometric ratio of the starting materials can only be achieved with  $[P_{66614}][Cl]$ , which becomes crucial when a single-phase product is desired (see next section). Both ILs can easily be recovered by distilling off the organic solvent used for product separation. However, in terms of yield, sustainability, and upscaling,  $[P_{66614}][Cl]$  is the better choice, as no significant loss occurs during reaction and recovery.

**Structural Analysis of  $Cu_{3-x}P$ .** The structure of  $Cu_{3-x}P$  was analyzed by Olofsson in 1972.<sup>27</sup> It crystallizes in the acentric hexagonal space group  $P6_3cm$  with one P atom and four Cu atoms in the asymmetric unit. The coordination polyhedron of the P atom is a trigonal prism with capping atoms on all faces. The coordination of Cu(1) and Cu(2) by P atoms is distorted tetrahedral; in the case of Cu(3) and Cu(4) it is distorted trigonal.

More interestingly, the structure can be subdivided into layers. The copper atoms in trigonal coordination are the nodes in a honeycomb net parallel to (001). The rings of this net are buckled, but the Cu–P distances are very similar (235.1 to 236.7 pm). The tetrahedrally coordinated copper atoms are connecting these layers along the  $c$ -axis, but it is worth mentioning that some of the Cu–P distances are even shorter (234.4 to 296.6 pm) than those found in the rings (Figure 4).

As mentioned previously, Olofsson described how the sub-stoichiometry of  $Cu_{3-x}P$  manifests itself in partially occupied Cu(1) and Cu(2) positions.<sup>27</sup> de Trizio et al. recently further substantiated the experimental evidence by DFT calculations, which showed a negative value of the free energy of vacancy formation at the Cu(1) and Cu(2) positions.<sup>29</sup> With decreasing copper content, the number of tetrahedrally coordinated Cu atoms between the honeycomb layers is reduced, giving the compound a more layered character. This is consistent with the results of Schlenger et al., who observed a contraction of the unit cell while lowering the copper content.<sup>28</sup> This contraction, however, does not occur predominantly along the  $c$ -axis.

Although our results in general agree with those of Olofsson and Schlenger et al., some minor additions concerning the homogeneity range were noted. Single-phase samples of stoichiometric  $Cu_3P$  could not be obtained; all attempts to achieve this composition resulted in elemental copper as a byproduct instead. The Cu byproduct vanishes for ratios Cu/P

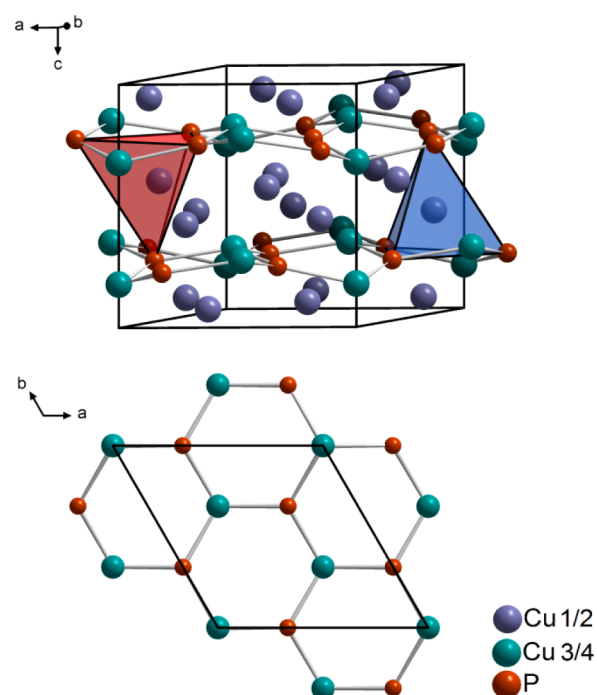


**Figure 4.** (top) The crystal structure of  $Cu_{3-x}P$  according to Olofsson.<sup>27</sup> Bonds between Cu(1)/(2) and P are omitted. Coordination of Cu(1) and Cu(2) is visualized with a blue and a red polyhedron, respectively. (bottom) Projection of the honeycomb net. The Cu(1) and Cu(2) atoms are omitted.

$\leq 2.95:1$ . EDX of respective samples synthesized in  $[P_{66614}][Cl]$  (Figure S2 and Table S2, Supporting Information) led to the compositions  $Cu_{2.95(4)}P$ , supporting the hypothesis of an intrinsic sub-stoichiometry of  $Cu_{3-x}P$  under standard conditions, which is consistent with results of DFT calculations of de Trizio et al.<sup>29</sup>

To get an overview of the homogeneity range, samples with different nominal compositions of  $Cu_{3-x}P$  ( $x = 0, 0.05, 0.1, 0.2, \dots, 0.7$ ) were prepared. As already described, samples with nominal composition  $Cu_3P$  are known to contain residual copper, whereas those with a composition of  $Cu_{2.95}P$  are single-phase according to the results of PXRD and SEM/EDX measurements. EDX analyses of samples with higher phosphorus contents show fluctuations in the chemical composition, caused by the precipitation of a byproduct, most likely  $CuP_2$ , as revealed by EDX mappings and point analyses (see Figures S3–S5 and Table S3, Supporting Information). However, X-ray powder diagrams show no  $CuP_2$  reflections either due to the small amount of the byproduct or due to an inferior crystallinity of the precipitates.  $CuP_2$  precipitate formation has already been observed for samples with a composition of  $Cu_{2.85}P$ .<sup>27</sup> According to our results the formation of a  $CuP_2$  precipitate already starts at a nominal composition of  $Cu_{2.9}P$ , so batches with  $x = 0.05$  are the only single-phase  $Cu_{3-x}P$  samples obtained and characterized in this work.

In the following,  $^{31}P$  MAS NMR spectroscopy and Le Bail analyses were made on the same batches already analyzed by SEM (Figure S6, Supporting Information). The NMR peaks show an asymmetric broadening, which can be attributed to the presence of different  $Cu_{3-x}P$  phases within one batch (Figure 5). However, no signals from the  $CuP_2$  precipitation were observed. More obvious is, however, the considerable peak shift

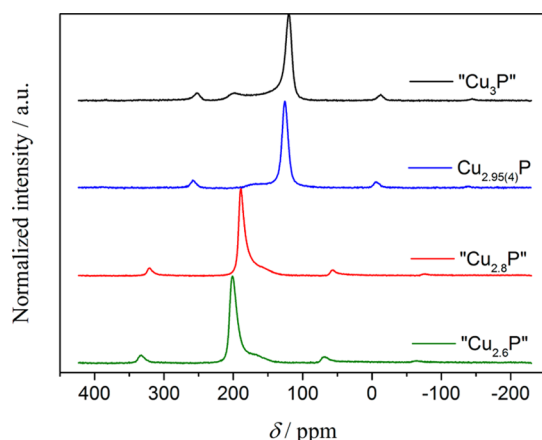


**Figure 5.**  $^{31}\text{P}$  MAS NMR spectra of  $\text{Cu}_{3-x}\text{P}$  with different nominal compositions synthesized in  $[\text{P}_{66614}][\text{Cl}]$ . Compositions given in quotation marks are nominal compositions.

going from copper-rich to copper-poor compositions. Comparing the nominal compositions  $\text{Cu}_3\text{P}$  and  $\text{Cu}_{2.95(4)}\text{P}$ , the shift of the main peak is negligible supporting the intrinsic substoichiometry of this compound again (Figure 5). The phosphorus-rich edge of the homogeneity range was found at an approximate composition of  $\text{Cu}_{2.6}\text{P}$ , which is slightly less than reported before ( $x = 0.3$ ).<sup>27,28</sup> The NMR signal of  $\text{Cu}_{3-x}\text{P}$ , shifts in total  $\sim 32$  ppm downfield between samples with nominal compositions of  $\text{Cu}_{2.9}\text{P}$  and  $\text{Cu}_{2.8}\text{P}$  (Figure 5). As already discussed in a previous work,  $\text{Cu}_{3-x}\text{P}$  is known to exhibit a Knight shift, which is considered as indicative for a conducting sample.<sup>34</sup> Thus, the considerable offset between the  $^{31}\text{P}$  signals of  $\text{Cu}_{2.9}\text{P}$  and  $\text{Cu}_{2.8}\text{P}$  indicates a strongly changed Knight shift. This means phosphorus-rich samples are expected to have enhanced electron mobility, that is, a higher conductivity. The chemical shift of the  $^{31}\text{P}$  signal correlates well with the change of the unit cell dimensions, which makes a proportional relation between both parameters probable (Figure 6; for detailed data see Table S4, Supporting Information).

It is worth mentioning that it was not possible to fit the diffraction pattern of a sample with the nominal composition  $\text{Cu}_3\text{P}$  with the hexagonal structure model satisfactorily due to a considerable broadening of the reflections. A possible distortion

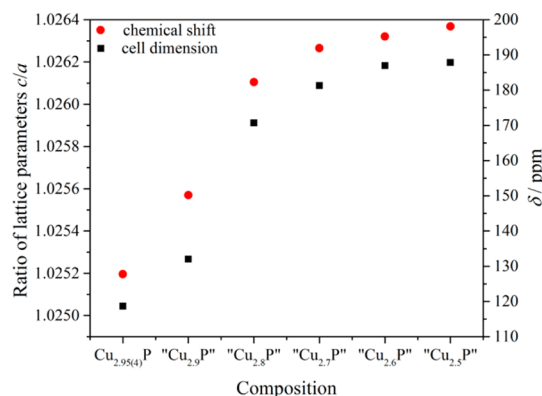


**Figure 6.** Correlation between chemical shift (center of gravity of the signal) and change of the cell dimension of samples with different compositions synthesized in  $[\text{P}_{66614}][\text{Cl}]$ . Compositions given in quotation marks are nominal compositions.

of the  $\text{Cu}_{3-x}\text{P}$  structure at its copper-rich limit must be investigated in the future by more elaborate experiments.

**Electronic Behavior.** The results of the solid-state NMR experiments indicate a metallic character of the  $\text{Cu}_{3-x}\text{P}$  material. Metallic conductivity of  $\text{Cu}_{3-x}\text{P}$  was proposed by Robertson et al., who measured a low electrical resistance on a single crystal.<sup>33</sup> However, semiconducting behavior was claimed by several other groups.<sup>29–31</sup> To shed some light on the electronic properties the band structure of idealized stoichiometric  $\text{Cu}_3\text{P}$  was calculated (Figure 7). According to these calculations, even the copper-rich boundary phase should be metallic.

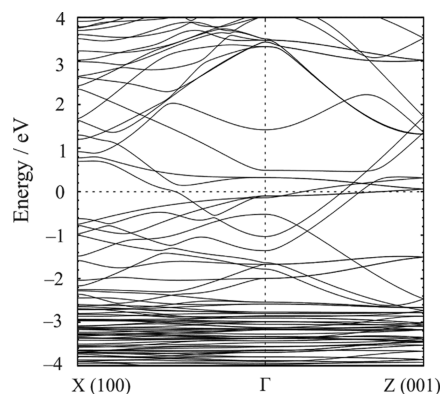


**Figure 7.** Band structure of  $\text{Cu}_3\text{P}$  on the basis of the structure reported by Olofsson.<sup>27</sup>

To corroborate the theoretical results, the temperature-dependent resistance of a sample with the composition  $\text{Cu}_{2.95(4)}\text{P}$  was measured. The sample shows metallic behavior as the resistance decreases monotonically with decreasing temperature to 4 K (Figure S7, Supporting Information). Likewise, Hall measurements at 300 K evidence a carrier density of  $\sim 1 \times 10^{27}$  carriers per cubic meter, which is in the same range as those for the alkali metals, for example.<sup>55</sup>

## CONCLUSION

Microcrystalline  $\text{Cu}_{3-x}\text{P}$  can be synthesized by using an ionothermal synthesis route most efficiently in the ionic liquid  $[\text{P}_{66614}][\text{Cl}]$ . The starting materials, copper metal and red phosphorus, are readily available and practically nontoxic. The IL-based approach significantly simplifies the experimental procedure, because no autogenous pressure is generated. A common glass flask with stopper is sufficient as reaction vessel, making it easy to avoid contamination by air and moisture.  $[\text{P}_{66614}][\text{Cl}]$  promotes the reaction but is neither affected by the starting material nor degenerates thermally within the reaction cycle and is, thus, easily recyclable without influence on the overall phosphorus efficiency. Yields of single-phase  $\text{Cu}_{2.95(4)}\text{P}$  close to 100% were obtained. Our results confirm that a phase of the precise composition  $\text{Cu}_3\text{P}$  probably does not exist. Bulk  $\text{Cu}_{2.95(4)}\text{P}$  is metallic. Solid-state NMR spectroscopy revealed the possibility of enhanced electron mobility in phosphorus-rich samples of  $\text{Cu}_{3-x}\text{P}$ .

## ASSOCIATED CONTENT

### Supporting Information

The Supporting Information is available free of charge on the ACS Publications website at DOI: 10.1021/acs.inorgchem.6b01397.

SEM images of  $\text{Cu}_{3-x}\text{P}$ , EDX data for  $\text{Cu}_{2.95(4)}\text{P}$ , data of elemental analysis of  $\text{Cu}_{3-x}\text{P}$ , solid-state NMR data, results of lattice parameter fitting, temperature-dependent resistance of  $\text{Cu}_{2.95(4)}\text{P}$  (PDF)

## AUTHOR INFORMATION

### Corresponding Author

\*E-mail: [thomas.doert@tu-dresden.de](mailto:thomas.doert@tu-dresden.de).

### Author Contributions

All authors have given approval to the final version of the manuscript.

### Notes

The authors declare no competing financial interest.

## ACKNOWLEDGMENTS

We would like to thank P. Nockemann (Queen's Univ, Belfast) for helpful discussions. We gratefully acknowledge G. Auffermann (MPI CPFS, Dresden) for elemental analysis, I. Veremchuk (MPI CPFS, Dresden) for SPS, A. Brünner (TU, Dresden) for help on SEM and EDX measurements, A. Isaeva (TU, Dresden) for band structure calculations, and S. Yogendra (TU, Dresden) for measuring NMR spectra. We thank the Deutsche Forschungsgemeinschaft for financial support within the Priority Program SPP1708.

## REFERENCES

- Steen, I. *Phosphorus Potassium* **1998**, 227, 25–31.
- Smil, V. *Annu. Rev. Energy Environ.* **2000**, 25, 53–88.
- Schröder, J. J.; Cordell, D.; Smit, A. L.; Rosemarin, A. *Sustainable Use of Phosphorus*, EU Tender ENV.B.1/ETU/2009/0025; Plant Research International Wageningen UR: Wageningen, Netherlands, 2010.
- Van Vuuren, D. P.; Bouwman, A. F.; Beusen, A. H. W. *Global Environ. Chang.* **2010**, 20, 428–439.
- Cordell, D.; Drangert, J. O.; White, S. *Global Environ. Chang.* **2009**, 19, 292–305.
- Cordell, D.; White, S. *Sustainability* **2011**, 3, 2027–2049.
- Von Schnering, H. G.; Hönle, W. *Chem. Rev.* **1988**, 88, 243–273.
- Pöttgen, R.; Hönle, W.; von Schnering, H. G. Phosphides: Solid-State Chemistry. In *Encyclopedia of Inorganic Chemistry*, 2nd ed.; King, R. B., Ed.; John Wiley & Sons, Ltd: Chichester, U.K., 2005; Vol. 8, pp 4255–4308.
- Bawohl, M.; Nilges, T. *Z. Anorg. Allg. Chem.* **2015**, 641, 304–310.
- Muetterties, E. L.; Sauer, J. C. *J. Am. Chem. Soc.* **1974**, 96, 3410–3415.
- Brock, S. L.; Perera, S. C.; Stamm, K. L. *Chem. - Eur. J.* **2004**, 10, 3364–3371.
- Oyama, S. T.; Gott, T.; Zhao, H.; Lee, Y. K. *Catal. Today* **2009**, 143, 94–107.
- Prins, R.; Bussell, M. E. *Catal. Lett.* **2012**, 142, 1413–1436.
- Bhushan, M.; Catalano, A. *Appl. Phys. Lett.* **1981**, 38, 39–41.
- Nayar, P. S.; Catalano, A. *Appl. Phys. Lett.* **1981**, 39, 105–107.
- Luber, E. J.; Mobarok, M. H.; Buriak, J. M. *ACS Nano* **2013**, 7, 8136–8146.
- Shirotani, I.; Takaya, M.; Kaneko, I.; Sekine, C.; Yagi, T. *Phys. C* **2001**, 357–360, 329–332.
- Bachmann, K. J. *Annu. Rev. Mater. Sci.* **1981**, 11, 441–484.
- Bera, D.; Qian, L.; Tseng, T. K.; Holloway, P. H. *Materials* **2010**, 3, 2260–2345.
- Preusse, H.; Bolton, J. D. *Powder Metall.* **1999**, 42, 51–62.
- Nikanorov, S. P.; Peller, V. V. Continuous Casting Design by the Stepanov Method. In *Handbook of Metallurgical Process Design*; Totten, G. E., Funatani, K., Xie, L., Eds.; Marcel Dekker, Inc: Basel, Switzerland, 2004; pp 295–349.
- Kato, T.; Adachi, S.; Aoyagi, T.; Naito, T.; Yamamoto, H.; Nojiri, T.; Yoshida, M. *IEEE J. Photovoltaics* **2012**, 2, 499–505.
- Solovoyov, S. E. Oxygen Scavengers. In *Kirk-Othmer Encyclopedia of Chemical Technology*; Seidel, A., Bickford, M., Eds.; John Wiley and Sons, Inc: Hoboken, NJ, 2014; pp 1–31.
- Pfeiffer, H.; Tancret, F.; Brousse, T. *Electrochim. Acta* **2005**, 50, 4763–4770.
- Chandrasekar, M. S.; Mitra, S. *Electrochim. Acta* **2013**, 92, 47–54.
- Stan, M. C.; Klöpsch, R.; Bhaskar, A.; Li, J.; Passerini, S.; Winter, M. *Adv. Energy Mater.* **2013**, 3, 231–238.
- Olofsson, O.; et al. *Acta Chem. Scand.* **1972**, 26, 2777–2787.
- Schlenger, H.; Jacobs, H.; Juza, R. *Z. Anorg. Allg. Chem.* **1971**, 385, 177–201.
- De Trizio, L.; Gaspari, R.; Bertoni, G.; Kriegel, I.; Moretti, L.; Scotognella, F.; Maserati, L.; Zhang, Y.; Messina, G. C.; Prato, M.; Marras, S.; Cavalli, A.; Manna, L. *Chem. Mater.* **2015**, 27, 1120–1128.
- Manna, G.; Bose, R.; Pradhan, N. *Angew. Chem., Int. Ed.* **2013**, 52, 6762–6766; *Angew. Chem.* **2013**, 125, 6894–6898.
- Ann Aitken, J. A.; Ganzha-Hazen, V.; Brock, S. L. *J. Solid State Chem.* **2005**, 178, 970–975.
- De Trizio, L.; Figuerola, A.; Manna, L.; Genovese, A.; George, C.; Brescia, R.; Saghi, Z.; Simonutti, R.; Van Huis, M.; Falqui, A. *ACS Nano* **2012**, 6, 32–41.
- Robertson, D. S.; Snowball, G.; Webber, H. *J. Mater. Sci.* **1980**, 15, 256–258.
- Furó, I.; Bakonyi, I.; Tompa, K.; Zsoldos, É.; Heinmaa, I.; Alla, M.; Lippmaa, E. *J. Phys.: Condens. Matter* **1990**, 2, 4217–4225.
- Bichat, M.-P.; Politova, T.; Pfeiffer, H.; Tancret, F.; Monconduit, L.; Pascal, J.-L.; Brousse, T.; Favier, F. *J. Power Sources* **2004**, 136, 80–87.
- Carenco, S.; Hu, Y.; Florea, I.; Ersen, O.; Boissière, C.; Mézailles, N.; Sanchez, C. *Chem. Mater.* **2012**, 24, 4134–4145.
- Su, H. L.; Xie, Y.; Li, B.; Liu, X. M.; Qian, Y. T. *Solid State Ionics* **1999**, 122, 157–160.
- Xie, Y.; Su, H. L.; Qian, X. F.; Liu, X. M.; Qian, Y. T. *J. Solid State Chem.* **2000**, 149, 88–91.
- Liu, S.; Qian, Y.; Xu, L. *Solid State Commun.* **2009**, 149, 438–440.
- Cooper, E. R.; Andrews, C. D.; Wheatley, P. S.; Webb, P. B.; Wormald, P.; Morris, R. E. *Nature* **2004**, 430, 1012–1016.
- Parnham, E. R.; Drylie, E. A.; Wheatley, P. S.; Slawin, A. M. Z.; Morris, R. E. *Angew. Chem., Int. Ed.* **2006**, 45, 4962–4966; *Angew. Chem.* **2006**, 118, 5084–5088.
- Parnham, E. R.; Morris, R. E. *J. Am. Chem. Soc.* **2006**, 128, 2204–2205.
- Parnham, E. R.; Morris, R. E. *Acc. Chem. Res.* **2007**, 40, 1005–1013.
- Morris, R. E. *Chem. Commun.* **2009**, 2990–2998.
- Brauer, G. *Handbuch Der Präparativen Anorganischen Chemie*, 3rd ed.; F. Enke: Stuttgart, 1962.
- Fana2006, The Crystallographic Computing System; Institute of Physics: Praha, Czech Republic, 2015 Petricek, V.; Dusek, M.; Palatinus, L. *Z. Kristallogr. - Cryst. Mater.* **2014**, 229, 345–352.
- The Elk FP-LAPW Code, version 1.4.22, 2009–2015; Online: <http://elk.sourceforge.net>.
- Groh, M. F.; Paasch, S.; Weiz, A.; Ruck, M.; Brunner, E. *J. Inorg. Chem.* **2015**, 2015, 3991–3994.
- Scheer, M.; Balázs, G.; Seitz, A. *Chem. Rev.* **2010**, 110, 4236–4256.
- Dragulescu-Andrasi, A.; Miller, L. Z.; Chen, B.; McQuade, D. T.; Shatruk, M. *Angew. Chem., Int. Ed.* **2016**, 55, 3904–3908; *Angew. Chem.* **2016**, 128, 3972–3976.
- Kanatzidis, M. G.; Pöttgen, R.; Jeitschko, W. *Angew. Chem., Int. Ed.* **2005**, 44, 6996–7023; *Angew. Chem.* **2005**, 117, 7156–7184.
- Ionic Liquids in Synthesis*, 2nd ed.; Wasserscheid, P., Welton, T., Eds.; Wiley-VCH: Weinheim, Germany, 2008.
- Eckstein, N.; Hohmann, A.; Wehrich, R.; Nilges, T.; Schmidt, P. *Z. Anorg. Allg. Chem.* **2013**, 639, 2741–2743.

- (54) Henkes, A. E.; Vasquez, Y.; Schaak, R. E. *J. Am. Chem. Soc.* **2007**, *129*, 1896–1897.
- (55) Palenskis, V. *World J. Condens. Matter Phys.* **2013**, *3*, 73–81.